



Intervallence excitation of the Creutz–Taube ion. Resonance Raman and time-dependent scattering studies of Franck–Condon effects

Hong Lu, Vladimir Petrov¹, Joseph T. Hupp

Department of Chemistry, Northwestern University, Evanston, IL 60208, USA

Received 28 December 1994

Abstract

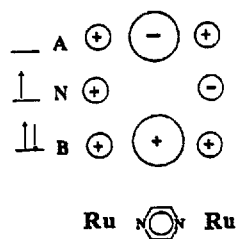
Franck–Condon effects associated with intervalence excitation of the Creutz–Taube ion (a prototypical delocalized mixed-valency system) have been evaluated via a time-dependent analysis of resonance Raman scattering intensities and the intervalence absorption lineshape. Quantitative studies in the extended near infrared (1320 nm excitation) revealed that at least eight, and possibly nine, vibrational modes are coupled to the intervalence transition. Numerical assessment of vibrational structural changes and reorganizational energy contributions showed that the most important modes, in a Franck–Condon sense, are metal–ligand stretches along the metal–bridge–metal axis (i.e. Ru–N(pyrazine) and trans-Ru–NH₃). Also active, however, are several pyrazine localized vibrations.

1. Introduction

The Creutz–Taube ion, (NH₃)₅Ru–pyrazine–Ru(NH₃)₅⁵⁺ (**1**), is an archetypal example of a class III (i.e. electronically delocalized) mixed-valence system [1–5]. As such, it represents one extreme in a continuum of systems related to bridge mediated electron transfer reactivity. System **1** is characterized spectroscopically by a nominally metal-to-ligand charge transfer transition in the visible region and by an intense, narrow ‘intervalence’ transition in the extended near infrared (i.e. a transition that would be metal-to-metal charge-transfer in character if the valences were localized). Recently we reported on preliminary resonance Raman studies (1320 nm exci-

tation) of the lower energy transition [6]. From the studies we concluded (consistent with recent theoretical work [7–10]) that the electronic ground state of **1** is characterized by three-center bonding (see Scheme 1) and that mixing of one or more pyrazine π^* orbitals with the available pair of Ru d_{xy} orbitals is the operative mechanism for delocalization. We also concluded that the intervalence transition is reasonably well described as a three-center bonding orbital (B) to two-center nonbonding orbital (N) excitation, as previously suggested on the basis of theoretical studies [7–10]. (Our studies are also consistent with more sophisticated models that additionally invoke pyrazine(π)/ruthenium($d\pi$) orbital interactions [11,12].) The Raman findings were inconsistent, however, with standard two-site (two-state) descriptions of electronic delocalization and intervalence excitation [13–15].

¹ Permanent address: S.I. Vavilov State Optical Institute, St. Petersburg, Russian Federation.



Scheme 1.

Further consideration of the simple model in Scheme 1 suggests that charge should be transferred from the bridging ligand to both metal centers upon intervalence excitation. Consistent with that idea, the Ru–N(pyrazine) stretch and several totally symmetric modes of pyrazine itself are coupled to the intervalence transition as shown directly by resonance Raman enhancement effects [6]. In principle, the intensities of such modes (together with the electronic absorption spectrum) contain quantitative information about the vibrational structural changes accompanying excited state formation [16–20]. We have now obtained corrected resonance Raman scattering intensities for eight vibrations (relative intensities). We have analyzed these by time-dependent wavepacket propagation methods [16–18] to obtain detailed numerical estimates for vibrational displacement parameters and internal reorganizational parameters (Franck–Condon information). The new results provide a quantitative basis for understanding how vibronic coupling affects intervalence excitation of 1 . To the best of our knowledge, this is the first such experimental study for a valence delocalized system.

2. Experimental

Resonance Raman measurements were made on a Spex 1403 double monochromator containing gratings blazed at 1200 nm (600 groove/mm). Scattered light was monitored with a liquid nitrogen cooled germanium detector (4 mm × 4 mm; North Coast model E0817L) coupled to a Stanford Instruments model SR530 lock-in amplifier. The excitation source was a Nd:YAG laser (Lee Laser model 712ST) configured to operate at both 1320 and 1337 nm. Typical powers were 1.1 and 0.7 W for the shorter and longer wavelengths, respectively. The output

was mechanically chopped prior to sample irradiation; however, no attempt was made to separate the two excitation colors. Consequently, scattering peaks were duplicated with 110 cm^{-1} separation in experimental spectra.

Dilute (≈ 1.5 to 4 mM) samples of the mixed valence ion were prepared in nitromethane- d_3 (or occasionally acetonitrile- d_3) by oxidizing $[(\text{NH}_3)_5\text{Ru-pyrazine-Ru}(\text{NH}_3)_5](\text{PF}_6)_4$ with Br_2 (or occasionally $[\text{Fe}(\text{bpy})_3](\text{PF}_6)_3$). Perdeuterated solvents were used so that C–H overtone based solvent self-absorption effects could be avoided. Dissolved samples were irradiated in a spinning NMR tube (90° geometry) while cooling with a stream of nitrogen. (The mixed-valence ion is photo inert in the near infrared; however, extensive thermal degradation occurs within a few minutes if cooling is omitted.)

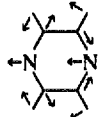
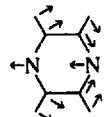
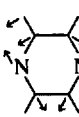
Raman spectra were corrected for frequency-dependent variations in instrument throughput and detector response by calibrating the overall response with an approximate black body source (100 W quartz halogen lamp (Epply Laboratory, Inc.); Power Ten model 3300B-4015 power supply designed for spectral calibration).

Electronic absorption spectra were obtained with a CARY 14 spectrophotometer that had been rebuilt and computerized by OLIS.

3. Results

Excitation of 1^{5+} at 1320 nm yielded resonance enhanced scattering from eight vibrational modes (see Table 1). (That scattering was enhanced was established by performing additional experiments with 1064 nm excitation (post resonant) and by examining 1^{4+} and 1^{6+} (nonchromophoric in the near infrared).) Five of the eight vibrations were observed previously [6] and, indeed, the new spectra closely resemble our earlier results. Improvements in signal-to-noise (based on improved collection efficiencies and better rejection of Rayleigh scattering) permitted the detection of new Raman peaks at 262 and 1232 cm^{-1} . The former has been assigned in related compounds as an $\text{NH}_3\text{-Ru-NH}_3$ bending mode [20]. It is difficult, however, to see why a bending mode would be coupled to an intervalence transition. A more probable assignment here and in our earlier work is an Ru– NH_3 stretch for the bond

Table 1
Vibrational frequencies, scattering intensities and Franck–Condon parameters for intervalence excitation of the Creutz–Taube ion

Frequency (cm ⁻¹)	Relative intensity ^a	Calculated displacement ^b	χ_k^c (cm ⁻¹)	Assignment
262	0.55	1.29	220	Ru–NH ₃ (axial)
324	0.83	1.26	260	Ru–N(pyraz)
697	1.00	0.53	100	ν_{6a} : 
1004	0.62	0.25	30	ν_1 : 
1078	0.41	0.18	18	ν_{18a} : 
1232	0.25	0.11	8	ν_{9a} : 
1316	0.35	0.12	10	ν_{19a} : 
1412	d	0.21 ^e	30	ν_{14} : 
1596	≤ 0.5 ^f	0.10 ^e	9	ν_{9a} : 

^a Integrated corrected scattering intensity, relative to peak intensity at 697 cm⁻¹.

^b Determined from absorption spectrum and corrected scattering spectrum by using Eqs. (1)–(3).

^c Single mode contribution to vibrational reorganization energy, calculated from Eq. (4).

^d Intensity is poorly defined, but clearly large in comparison with other high frequency modes.

^e Calculated value is based on optimal fit of the absorption spectrum only (i.e. experimental Raman scattering intensity was not fit).

^f Intensity is poorly defined; upper limit estimate is reported.

located trans to the bridge (i.e. axial position). The peak at 1232 cm⁻¹ is almost certainly a totally symmetric vibration of the bridging ligand [21,22]. The third new peak (1412 cm⁻¹) is, in retrospect,

also present in earlier spectra, but is obscured by a solvent mode. This feature is readily observable, however, when CD₃NO₂ is replaced by CD₃CN as solvent. It is tentatively assigned as a nontotally symmetric mode of pyrazine (see below). (An alternative assignment would be a symmetrical bending mode of the isolated axial NH₃ ligand.)

Also identified as a nontotally symmetric mode of pyrazine is a peak at 1316 cm⁻¹ [21,22]. Based in part on its low intensity, we previously suggested that it might be a combination band [7]. The band also appears in the intervalence enhanced Raman spectrum of trans a substituted analogue of the Creutz–Taube ion, but with an intensity much too high to accommodate the assignment as a combination mode [23].

Finally, evidence for a ninth mode (1596 cm⁻¹) was intermittently obtained. A peak at 1596 cm⁻¹ is readily observed with 1064 nm excitation (nonresonant excitation). With 1320 nm excitation, however, the Stokes shift is sufficient to place the peak at the red edge of the germanium detection window, where sensitivity is greatly diminished. We are unable to establish with certainty, therefore, the validity of the observation.

As indicated above, the detector sensitivity displays a significant wavelength or energy dependence over the range of interest in our experiment. That dependence, together with grating efficiency effects, is illustrated in Fig. 1 where the *overall* instrument response to a black body source is presented. The sharp features in the response curve (curve (1)) are artifacts associated with light absorption by water vapor; these are eliminated (curve (2)) when the spectrometer is flushed with dry nitrogen. In any case, correction for the instrument response and elimination of the spurious absorption leads to the corrected Raman scattering intensities shown in Fig. 2. Interestingly, one of the narrow features in the water vapor spectrum is coincident with a somewhat broader scattering peak at 324 cm⁻¹. The coincidence accounts for the previously reported splitting of this mode [6].

4. Analysis

Relative intensities in the absorption and resonance Raman spectra are directly related to frequen-

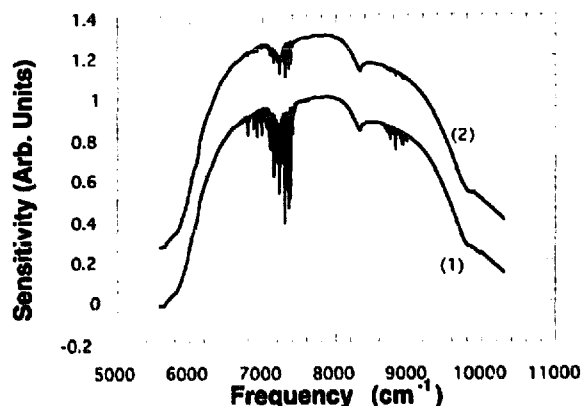


Fig. 1. Raman instrument response curve in: (1) air containing water vapor, and (2) a nominally dry nitrogen atmosphere (offset for clarity).

cies of vibrational modes and to the displacements these modes suffer in the electronic excited state. The time-dependent theory of spectroscopy [16,17] clearly addresses the relationships. In this theory, a vibrational wave packet that evolves in time is assumed to characterize the upper state excitation. The overlap between the initial packet Φ_k on the ground state surface and the dynamically evolving packet $\Phi_k(t)$ on the excited state surface is defined by $\langle \Phi_k | \Phi_k(t) \rangle$, such that [16–18]

$$\langle \Phi | \Phi(t) \rangle = \exp \left(\sum_k \left\{ -\frac{1}{2} \Delta_k^2 [1 - \exp(-i\omega_k t)] - \frac{1}{2} i\omega_k t - iE_{00}t - \Gamma^2 t^2 \right\} \right) \quad (1)$$

In this equation, t is time, E_{00} is the electronic energy gap, Γ is an empirical damping factor and Δ_k is the unitless normal coordinate displacement (see Fig. 3). The absorption cross section at frequency ω is given by

$$I(\omega) = \omega \int_{-\infty}^{\infty} e^{i\omega t} \langle \Phi | \Phi(t) \rangle dt. \quad (2)$$

Thus, Eq. (1) for the time-dependent vibrational overlap can be utilized (Eq. (2)) to give the absorption spectrum for any set of ω_k , Δ_k , E_{00} and Γ values.

The Raman cross section can be written as

$$R(\omega) = \int_0^{\infty} e^{i\omega t} \langle \Phi_R | \Phi(t) \rangle dt, \quad (3)$$

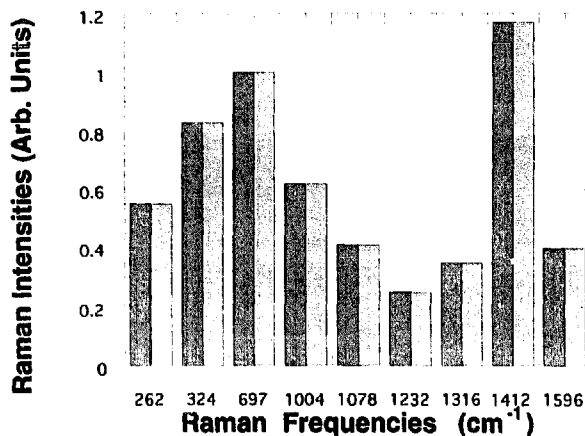


Fig. 2. Corrected experimental Raman scattering intensities (shaded bars) and calculated Raman scattering intensities (solid bars) for 1^5+ based on 1320 nm excitation. (Note that because scattering intensities at 1412 and 1596 cm^{-1} are poorly defined experimentally, these are arbitrarily equated with calculated intensities.)

where the overlap is then between the time-evolving wave packet on the upper surface and the final Raman vibrational state Φ_R on the ground surface. The half Fourier transform of this overlap gives the Raman spectrum. Following the general computational strategy described by Zink and Shin [18], we constructed programs for simulating the absorption lineshape and relative Raman scattering intensities. The aim of the simulation/data analysis was to determine absolute ground-state and intervalence-ex-

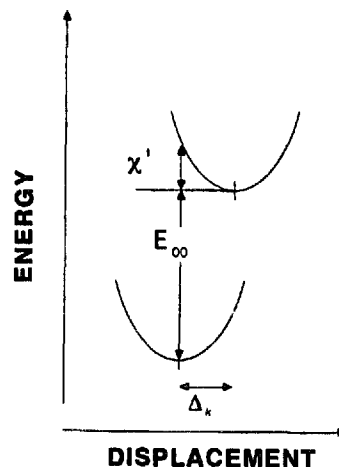


Fig. 3. Schematic illustration of relationships between displacement, energy and spectral parameters.

cited state vibrational structural changes. The analysis consisted of three processes: (1) calculation of a Raman excitation profile for each resonantly enhanced mode; (2) adjustment of the displacement for each mode to fit the observed scattering intensity (relative intensity) with 1320 nm excitation, and (3) scalar adjustment of the calculated set of displacements to fit the intervalence absorption lineshape. The final step (after iteration and consistency checks) unambiguously yields an absolute value of the unitless coordinate displacement for each vibrational mode.

In the analysis, Γ ($= 250 \text{ cm}^{-1}$) was assigned the smallest value that yielded smooth simulated Raman excitation profiles. $E_{(0)}$ was initially estimated as 6100 cm^{-1} (absorption maximum), but subsequently was adjusted to 5740 cm^{-1} to achieve the best fit of the absorption spectrum. Initial guesses for displacements for the first seven Raman active modes were based on the expected approximate proportionality between scattering intensities and Δ_k^2/ω_k^2 [16–18]. In view of the poorly defined intensities for the eighth (1412 cm^{-1}) and ninth (1596 cm^{-1}) modes, their displacements were treated largely as adjustable parameters. The final calculated displacements are listed in Table 1. The ability of the final parameters to reproduce the experimental scattering spectrum is illustrated in Fig. 2. A similar comparison for the absorption spectrum is shown in Fig. 4.

With estimates for Δ_k in hand it is additionally possible, via the following equation, where $\nu = \omega/2\pi$:

$$\chi'_k = \frac{1}{2} \Delta_k^2 \nu_k, \quad (4)$$

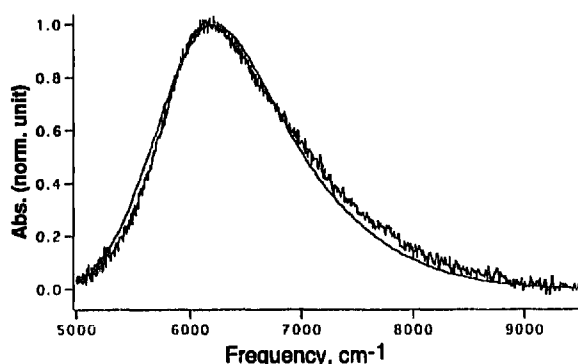


Fig. 4. Experimental and calculated electronic absorption spectra for 1^{5+} in CD_3NO_2 as solvent.

to obtain estimates for single-mode contributions (χ'_k) to the total vibrational reorganization energy (or optical Franck–Condon barrier). These are listed in Table 1.

5. Discussion

Calculated displacement parameters yield an excellent fit to the experimental Raman spectrum and a good, but imperfect, fit to the electronic absorption spectrum. In principle, any of several factors might be responsible for deviations in the latter, including: (1) Franck–Condon activity in vibrational modes beyond the range of our current detector (although no candidate modes are suggested by studies with (nonresonant) 1064 nm excitation); (2) neglect of finite temperature effects (presumably important only for the two lowest frequency modes) [24]; (3) neglect of vibrational anharmonicity (probably reasonable, however, given the very small magnitudes of the Δ_k values), (4) neglect of mode-mixing (Duschinsky rotation) and vibrational frequency changes in the upper electronic state [25], and (5) neglect of possible structure in Raman excitation profiles (potentially leading to errors in estimates of Franck–Condon activity). We hope to be able to address (1) and (5) shortly via tunable laser studies (1550–1800 nm; CoMgF source) involving indium–arsenide detection.

Another potential source of error is the (possibly) incorrect treatment of nontotally symmetric pyrazine modes. The appearance of these modes implies either a slight reduction in symmetry in the electronic ground state (and therefore a very slight degree of charge imbalance in the nominally fully delocalized assembly) or a slight change in symmetry upon formation of the electronic excited state. If the former explanation is correct, then the three modes which are nontotally symmetric with respect to free pyrazine will, nevertheless, be totally symmetric vibrations of 1^{5+} – and the analysis implied by Eqs. (1)–(4) will be correct. If the latter explanation is correct, then Δ_k (for these modes) cannot be obtained from Eqs. (1)–(3); nor can their contributions to the absorption lineshape (Eq. (2)) be accurately assessed. Instead an analysis along the lines pro-

posed by Zink et al. [18,26] and earlier by Johnson and Kinsey [27] would be required. In any case, the significance of the nontotally symmetric modes is small here.

One of the more striking findings from the analysis is the diversity of vibrations exhibiting Franck–Condon activity; at least eight, and more probably nine, are active. For obvious reasons, preliminary theoretical descriptions (three-site models [7–12]) have tended to emphasize dominant activity in a single mode (the ν_{6a} mode of pyrazine; see Table 1), although ancillary activity in Ru–N(py₂) and trans-Ru–NH₃ stretching modes has sometimes been suggested [10,12]. Interestingly, the time-dependent analysis indicates that the ν_{6a} mode (697 cm⁻¹), while prominent in the Raman spectrum and evidently the most important of the seven active pyrazine modes, is relatively unimportant in a Franck–Condon sense. Instead, the largest normal coordinate displacements and the largest reorganizational energy effects are associated with metal–ligand modes. Nevertheless, even these modes display only modest Δ and χ'_k values.

From Table 1, the total vibrational reorganization energy is estimated as ≈ 700 cm⁻¹. Given the magnitude of the E_{00} value required by the three-site theories and by the preceding spectral analysis, the 'intervalence' excited state in **1** is a strongly inverted or nested state (see Fig. 3; recall that in the three site model the intervalence transition acquires significant ligand to (double) metal charge transfer character). Conceivably with such small Δ_k values (especially for high frequency modes) nonradiative decay from the upper state could be relatively slow (despite the marginal energy gap). This raises the interesting possibility that structurally symmetrical delocalized mixed-valence systems might be capable of collecting and storing near infrared photons (solar radiation) for chemically useful amounts of time (e.g. nanoseconds, if subsequent photo redox reactivity were envisioned).

Finally, in related resonance Raman studies we have found that very extensive redistribution of Franck–Condon activity can accompany both symmetrical (trans) ligand substitution and unsymmetrical crown binding (second sphere association). Quantitative analysis of the vibrational structural changes should offer some insight into corresponding absorp-

tion lineshape and electronic structural changes [28]. We hope to report on these studies shortly.

Acknowledgement

We thank Laba Karki for supplying samples of the Creutz–Taube ion. We gratefully acknowledge the US Department of Energy, Office of Energy Research, Division of Chemical Sciences (Grant No. DE-FG02-87ER13808) for support of this research. JTH also gratefully acknowledges unrestricted support from the Dreyfus Foundation (Teacher–Scholar Award, 1991–96).

References

- [1] C. Creutz and H. Taube, *J. Am. Chem. Soc.* 91 (1969) 3988.
- [2] C. Creutz and H. Taube, *J. Am. Chem. Soc.* 95 (1973) 1086.
- [3] C. Creutz and M.H. Chou, *J. Inorg. Chem.* 26 (1987) 2995.
- [4] U. Furholz, H.B. Burgi, F.E. Wagner, A. Stebler, J.H. Ammeter, E. Krausz and R.J.H. Clark, *J. Am. Chem. Soc.* 106 (1984) 121.
- [5] D. Oh and S.G. Boxer, *J. Am. Chem. Soc.* 112 (1990) 8161.
- [6] V. Petrov, J.T. Hupp, C. Mottley and L.C. Mann, *J. Am. Chem. Soc.* 116 (1994) 2171.
- [7] L.T. Zhang, J. Ko and M.J. Ondrechen, *J. Am. Chem. Soc.* 109 (1987) 1666.
- [8] J. Ko and M.J. Ondrechen, *J. Am. Chem. Soc.* 107 (1985) 6161.
- [9] L.J. Root and M.J. Ondrechen, *Chem. Phys. Letters* 93 (1982) 421.
- [10] M.J. Ondrechen, S. Gozashti, L.-T. Zhang and F. Zhou 226 (1990) 225.
- [11] S.B. Piepho, *J. Am. Chem. Soc.* 110 (1988) 6319.
- [12] S.B. Piepho, *J. Am. Chem. Soc.* 112 (1990) 4197.
- [13] S.B. Piepho, E.R. Krausz and P.N. Schatz, *J. Am. Chem. Soc.* 100 (1978) 6319.
- [14] K. Neuenschwander, S.B. Piepho and P.N. Schatz, *J. Am. Chem. Soc.* 107 (1985) 7862.
- [15] K. Prassides and P.N. Schatz, *J. Phys. Chem.* 93 (1989) 83.
- [16] D. Tannor and E.J. Heller, *J. Chem. Phys.* 77 (1982) 202.
- [17] E.J. Heller, R.L. Sundberg and D. Tannor, *J. Phys. Chem.* 86 (1985) 1822.
- [18] J.L. Zink and K.S.K. Shin, *Advan. Photochem.* 16 (1991) 119.
- [19] F. Markel, N.S. Ferris, I.R. Gould and A.B. Myers, *J. Am. Chem. Soc.* 114 (1992) 6208.
- [20] S.K. Doorn and J.T. Hupp, *J. Am. Chem. Soc.* 111 (1989) 1142.
- [21] R.C. Lord, A.L. Marston and F.A. Miller, *Spectrochim. Acta* 9 (1957) 113.

- [22] J.D. Simmons and K.K. Innes, *J. Mol. Spectry.* 14 (1967) 190.
- [23] V. Petrov, unpublished studies.
- [24] K.T. Schomacker and P.M. Champion, *J. Chem. Phys.* 90 (1989) 5982.
- [25] D.E. Morris and W.H. Woodruff, *J. Phys. Chem.* 89 (1985) 5795.
- [26] D.M. Preston, W. Guenter, A. Lechner, G. Gliemann and J.L. Zink, *J. Am. Chem. Soc.* 110 (1988) 5628.
- [27] B.R. Johnson and J.L. Kinsey, *J. Chem. Phys.* 87 (1987) 1525.
- [28] Y. Dong, D. Yoon and J.T. Hupp, *J. Am. Chem. Soc.* 116 (1993) 4379.